Journal of Photochemistry and Photobiology A: Chemistry 208 (2009) 154–158

Contents lists available at ScienceDirect

Journal of Photochemistry and Photobiology A: Chemistry

journal homepage: www.elsevier.com/locate/jphotochem

Synthesis and characterization of novel heteroleptic ruthenium sensitizer for nanocrystalline dye-sensitized solar cells

Radhakrishnan Sivakumar[a], Antonius. T.M. Marcelis[b], Sambandam Anandan[a,*]

[a] Nanomaterials and Solar Energy Conversion Lab, Department of Chemistry, National Institute of Technology, Trichy 620 015, India
[b] Laboratory of Organic Chemistry, Wageningen University, Dreijenplein 8, 6703 HB Wageningen, The Netherlands

ARTICLE INFO

Article history:
Received 18 April 2009
Received in revised form 21 July 2009
Accepted 9 September 2009
Available online 16 September 2009

Keywords:
2,6-Bis(pyrazol-1-yl)isonicotinate
Ruthenium complex
Photo-sensitizer
Fluorescence
Lifetime

ABSTRACT

A novel heteroleptic ruthenium complex of the type [Ru(bpin)(dcbpyH$_2$)Cl]Cl (where bpin is 2,6-bis(pyrazol-1-yl)isonicotinic acid and dcbpyH$_2$ is 4,4′-dicarboxy-2,2′-bipyridine) was synthesized and characterized for tuning the LUMO level of the ruthenium sensitizer to achieve greater stabilization in the excited state which keeps the excess energy to maintain high driving force for electron injection. The photovoltaic performance of this complex as photosensitizer in a nanocrystalline TiO_2-based solar cell was studied and its overall energy conversion efficiency was determined (1.9%).

1. Introduction

Fascination for the field of photoelectrochemistry and the dye sensitization by a family of ruthenium–polypyridyl complexes adsorbed on nanocrystalline TiO_2 have aroused considerable interest in the development of photovoltaic devices for energy transduction. The pioneering work of Grätzel et al. [1,2] in Ru(II) polypyridyl complexes resulted in very efficient sensitizers such as "N_3 dye" and "black dye" in sensitizing nanocrystalline TiO_2 semiconductors with high energy conversion efficiencies. Although Argazzi et al. [3] synthesized complexes with very low π^*-energy level ligands with enhanced spectral response at longer wavelengths, the poor conversion efficiency was accompanied by reduced electron injection yields into the conduction band of TiO_2. This is in contrast to the black dye, where absorption takes place in the near IR-region and the extended π-conjugation and symmetry of the terpyridine ligands as compared to bipyridine ligands result in higher energy conversion efficiencies. The key component that governs the spectral response of the complexes are polypyridine ligands with low lying π^* energy levels through which heterogeneous electron transfer takes place. Nonetheless, only a certain groups have concentrated on ruthenium terpyridyl complexes [4–8]. Islam et al. [9,10] had realized the effect of non-chromophoric strong σ-donating β-diketonato chelating ligands on the absorption and redox properties of the tricarboxy terpyridil ruthenium(II) complex. Most of these studies reveal that the ligand has to be designed in such a way that the LUMO of the complex could be sufficiently long lived to undergo heterogeneous electron or energy transfer processes. In a systematic approach, the terpyridine ligands can be replaced by 2,6-bis(pyrazolyl)pyridine, and consequently maintaining the redox property of ruthenium complexes [11]. These terdentate ligands are able to stabilize the excited state of the complex. Stergiopoulos et al. [12] confirmed this property by synthesizing heteroleptic ruthenium complexes incorporating bis(pyrazolyl)pyridine and dcbpyH$_2$ as ligands and study their application as photosensitizer of nanocrystalline TiO_2. The most interesting features of these types of complexes are the broad MLCT absorption in the visible region, the high molar extinction coefficient and the well defined reversible oxidation/reduction waves, all essential criteria for fabrication of regenerative solar cells. In general, electron donating groups will destabilize the metal-based HOMO more than they destabilize the ligand-based LUMO and therefore non-radiative decay will be facilitated. Our aim is to lower the ^{3}MLCT excited state by introducing electron-withdrawing substituents, hence a greater stabilization of the LUMO can be achieved [13]. Therefore, a new heteroleptic ruthenium(II) complex was designed, incorporating bis(pyrazolyl)pyridine with a carboxylic acid substituent on the pyridine ring as ligand for fine tuning the LUMO level to attain enhanced performance on photosensitization of semiconductor TiO_2.

* Corresponding author. Tel.: +91 431 2503639; fax: +91 431 2500133.
E-mail addresses: sanand99@yahoo.com, sanand@nitt.edu (S. Anandan).

1010-6030/$ – see front matter © 2009 Elsevier B.V. All rights reserved.
doi:10.1016/j.jphotochem.2009.09.009

2. Experimental

2.1. Materials

$RuCl_3 \cdot 3H_2O$, 4,4′-dimethyl-2,2′-bipyridine, citrazinic acid, pyrazole and $POBr_3$ and tetrabutylammonium hexafluorophosphate ($TBAPF_6$) were obtained from Aldrich, All other chemicals used were of reagent grade (Aldrich or Sigma) and were used without further purification.

2.2. Synthesis

2.2.1. Synthesis of [Ru(bpin)Cl_3]

$RuCl_3 \cdot 3H_2O$ (260 mg, 1.26 mmol) and 2,6-bis(pyrazol-1-yl)isonicotinic acid (255 mg, 1 mmol) were dissolved in absolute ethanol and the mixture was refluxed for 4 h. The dark brown precipitate that formed was then allowed to settle overnight at 5 °C. The resulting dark brown powder was washed with absolute ethanol and diethylether and air dried (yield 410 mg, 90%). Data analysis: IR (KBr) cm^{-1}: 3121 (w, C–H aromatic), 3110 (w, C–H aromatic), 1711 (m, ν(C=O)), 1232 (m, ν(CO)). The peaks in the region 1621–1408 cm^{-1}, corresponding to the C=C and C=N stretching vibrations.

2.2.2. Synthesis of [Ru(bpin)(dcbpyH_2)Cl]Cl

Ru(bpin)Cl_3 (195.3 mg, 0.422 mmol) and 4,4′-dicarboxylic acid 2,2′-bipyridine (134.3 mg, 0.55 mmol) were refluxed for 8 h in 40 ml of ethanol/water (3/1, v/v) containing LiCl (0.019 g) and triethylamine (0.1 ml) as a reductant. The hot solution was filtered through celite and the filtrate was concentrated to a few milliliters and was stored for 2 days at 5 °C. Then the solid material was filtered to obtain [Ru(bpin)(dcbpyH)Cl] (yield 241.5 mg, 90%). Addition of 2 ml of an aqueous solution of HCl (2 M) to a suspension of complex obtained above [Ru(bpin)(dcbpyH)Cl] in methanol (10 ml) and on constant stirring for 2 h at room temperature dissolves the precipitate and forms a new complex ([Ru(bpin)(dcbpyH_2)Cl]Cl). The complex is then precipitated by the addition of diethyl ether (20 ml). The resulting brown-black solid was then filtered and washed with diethyl ether and dried in an oven at 50 °C for 2 h (yield 240 mg, 85%).

Data analysis: UV–vis (in methanol), λ_{max} (ε, $10^4\ M^{-1}\ cm^{-1}$): 416 nm (2.97), 456 nm (2.95), 525 (1.03), 610 nm (0.3). IR (KBr Pellet) cm^{-1}: 3111 (m, C–H aromatic), 3100 (w, C–H aromatic), 2921 (w, C–H aliphatic), 2815 (w, C–H aliphatic), 1701 (m, ν(C=O)). The peaks in the region 1621–1408 cm^{-1}, corresponding to the C=C and C=N stretching vibrations. ^{1}H NMR (in CD_3OD) δ_{ppm}: $H_{1,11}$ = 9.4 (d), $H_{2,10}$ = 6.67 (m), $H_{3,9}$ = 7.59 (d), H_5 = 8.92 (s), H_7 = 8.80 (s), H_{12} = 7.68 (d), H_{13} = 7.43 (d), H_{15} = 9.14 (s), H_{18} = 9.28 (s), H_{20} = 8.40 (d), H_{21} = 10.34 (d). ESI-MS: m/z = 602.0 $[M-Cl]^+$ it can be assigned to the parent ion peak for [Ru(bpin)(dcbpyH_2)].

2.3. Characterization details

^{1}H NMR spectra were recorded with a Varian INOVA system 400 (MHz) spectrometer at 298 K with TMS as internal standard. UV–vis and fluorescence spectra were recorded in 1 cm path length quartz cell on a Perkin Elmer EZ301 spectrophotometer and Shimadzu RF-5301 PC spectrofluorophotometer, respectively. Electrochemical measurements were recorded in a conventional three electrode system using CHI-604C electrochemical analyzer. A platinum plate was used as counter electrode; glassy-carbon was employed as working electrode while silver wire was used as the quasi reference. The cyclic voltammagram of the complex was obtained by dissolving 2 mM of the solution in acetonitrile containing 0.1 M tetrabutylammonium hexafluorophosphate salt. FT-IR spectra were recorded by using a JASCO-460 plus model spectrometer using KBr pellet techniques. Fluorescence lifetime measurements were carried out in a picosecond time correlated single photon counting (TCSPC) spectrometer. The excitation source is the tunable Ti-sapphire laser (TSUNAMI, Spectra Physics, USA). The fluorescence decay was analyzed by using the software provided by IBH (DAS-6). Mass spectra were obtained by electrospray ionization technique using a Micromass Quattro II Triple-Quadrupole mass spectrometer.

2.4. Photovoltaic measurements

Nanocrystalline TiO_2 films were prepared on the conducting glass support ITO. Coating the TiO_2 surface with the dye was carried out by dipping the electrode (maintained at 80 °C) in a 3×10^{-4} M solution of the ruthenium complex in ethanol for 24 h. A deep yellow-brown color formed immediately after immersion of the glass plates and confirms the dye attachment on the semiconductor surface. After the dye adsorption was complete, the electrode was withdrawn from the solution and dried under a stream of argon. The regenerative photo-electrochemical cell was fabricated by sandwiching dye coated TiO_2 film with a thin platinum coated conductive glass support serves as counter electrode while iodine/iodide (0.3 M LiI and 0.03 M I_2) employing as redox electrolyte. The electrodes were clipped together and illuminated through the TiO_2-sensitized surface.

3. Results and discussion

The ligands 2,6-bis(pyrazol-1-yl)isonicotinic acid (bpin) and 4,4′-dicarboxy-2,2′-bipyridine (dcbpyH_2) were synthesized as described earlier by Vermonden et al. [14] and Garelli and Vierling [15]. First, [Ru(bpin)Cl_3] was prepared according to a procedure from literature [16]. Then, the new heteroleptic ruthenium(II) complex [Ru(bpin)(dcbpyH_2)Cl]Cl was synthesized by reaction of the dcbpyH_2 ligand with the precursor [Ru(bpin)Cl_3] in an ethanol/water (3:1) mixture containing Et_3N which acts as reducing and deprotonating agent and subsequent treatment with concentrated HCl. The complex is soluble in ethanol, methanol, acetonitrile, acetone and moderably soluble in $CHCl_3$. The synthesized complex is characterized by IR, NMR and Mass spectrometric analysis.

3.1. ^{1}H NMR spectra

Fig. 1 shows the structure of the novel ruthenium complex and its ^{1}H NMR spectrum in CD_3OD as a solvent. Complexation reduces the electron density of the ligands, which causes a deshielding

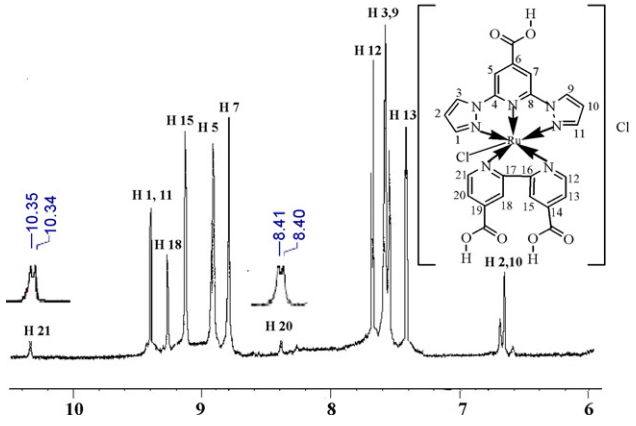

Fig. 1. The structure of the novel ruthenium complex and its NMR spectrum in CD_3OD.

effect on the resonance field and hence, the NMR spectrum of the title complex in solution shows all the peaks above 6 ppm. The four doublet and two singlet signals (δ_{ppm} = 7.68 (H_{12}), 7.43 (H_{13}), 8.40 (H_{20}), 10.34 (H_{21}), 9.14 (H_{15}), 9.28 (H_{18})) were attributed to the aromatic protons of the bipyridine moiety. The signal at δ = 10.34 ppm is due to the closer proximity of the corresponding hydrogen (H_{21}) to the chloride ligand. The two singlet signals (δ_{ppm} = 8.92 (H_5), 8.80 (H_7)) were assigned to the pyridinyl protons of the tridentate ligand. The pyrazolyl moiety protons show two doublet signal (δ_{ppm} = 9.4 ($H_{1,11}$) and 7.59 ($H_{3,9}$)). The signal at δ = 6.67 ppm ($H_{2,10}$) was due to the chemically equivalent pyrazolyl protons.

3.2. UV–vis and emission spectra

Fig. 2a shows the absorption spectrum of the novel ruthenium complex in methanol as a solvent. The UV region consists primarily of intense ligand-localized π–π^* transitions, by strong absorptions in the 220–305 nm range that can be assigned to intraligand transitions of the tridentate and bidendate ligand. The complex shows broad absorption bands in the visible region with two peak maxima at 416 nm (ε = 29,700 M^{-1} cm^{-1}) and 456 nm (ε = 29,500 M^{-1} cm^{-1}) generally assigned to MLCT absorptions for the ruthenium complexes. Also the absorption is extended to higher wavelengths as seen by a broad absorption in the 525–610 nm range, which is encouraging for absorbing less energetic photons and the effective transformation of a broad spectrum of visible light into electricity. Even at 610 nm the extinction coefficient is still high (3000 M^{-1} cm^{-1}), which is very much important for photosensitization processes. The complex exhibits luminescence at 637 nm when it is excited at 450 nm in methanol at 298 K and the lifetime was determined to be 7.1 ns (Fig. 2b and c). This emission is mainly attributed to the electron-withdrawing substituents on the bis(pyrazolyl)pyridine ring, whereas similar ruthenium sensitizers without electron-withdrawing substituents on 2,6-bis(pyrazolyl)pyridine do not show any emission [16–18]. The excitation spectrum (inset of Fig. 2b) of the complex shows a single peak at 554 nm which implies that the low energy absorption (456 nm) is emissive; this may be due to the fact that the primarily populated ^{1}MLCT is rapidly converted to ^{3}MLCT state which is responsible for the longer lifetime and radiative emission.

3.3. Electrochemistry

The cyclic voltammagram (Fig. 3a) of the complex shows reversible behaviour with a redox potential of 0.64 V vs. Ag/AgCl as reference electrode in a degassed acetonitrile solution containing 0.1 M n-Bu_4NPF_6. The redox behavior is attributed to the Ru^{II}/Ru^{III} redox couple. The redox potential for ruthenium sensitizers incorporating 2,6-bis(pyrazol-1-yl)pyridine without a carboxylate substituent is 0.73 V vs. Ag/AgCl [18]. The shift in the redox potential to less positive might be due to destabilization of the metal t_{2g} orbital upon introduction of the carboxylate group.

3.4. Photovoltaic performance

To evaluate the photovoltaic performance of the synthesized dye, photo-electrochemical cells were fabricated as reported earlier [19] and their power characteristics were determined using *I–V* measurements (Fig. 3b). Under solar irradiation (15 mW/cm^2), the fabricated photovoltaic cell produces a photo-voltage of 413 mV and a photo-current density of 2.1 mA/cm^2 with an overall solar energy conversion efficiency of 1.9%.As compared to earlier reports [16–18], the fabricated solar cell using our new heteroleptic sensitizer shows excellent performance. This is because the excited (^{3}MLCT) state, which is emissive in nature and keeps the excess energy to maintain a high driving force for electron injection

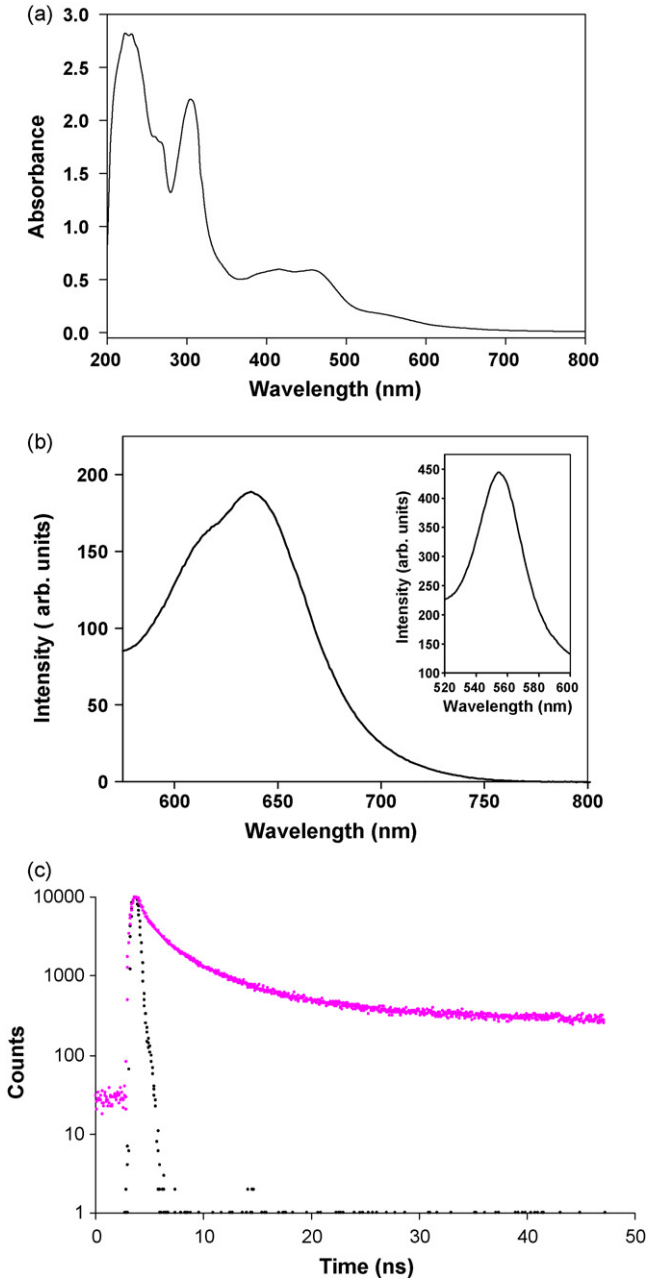

Fig. 2. (a) Absorption spectrum of the complex in methanol solution. (b) Fluorescence emission spectrum (λ_{emi} = 637 nm when excited at 450 nm) and excitation spectrum (λ_{exi} = 554 nm detected with emission wavelength of 637 nm) (inset) of the complex in methanol solution at room temperature. (c) Time-resolved emission decay of the complex in de-aerated methanol solution with 450 ± 2 nm pulsed excitation.

(Fig. 3c). Generally in ruthenium complexes, non-radiative emissions (energy dissipation through vibrational relaxations) was accompanied by the low lying triplet ligand field (LF) states which competes with interfacial electron transfer thus suppressing the electron injection yield [20]. But in the heteroleptic ruthenium complexes, due to radiative emission, the excited state energy provides thermodynamic force for electron injection. The presence of electron-withdrawing substituent in terdendate ligand stabilizes the LUMO of the sensitizer and plays a main role herein for achieving high energy conversion efficiencies. The sensitizer shows good absorptive property compared to the other standard dyes; i.e., covers entire part of the visible region and hence favorable for fabrication of photovoltaic device. However, the lower photo-voltage

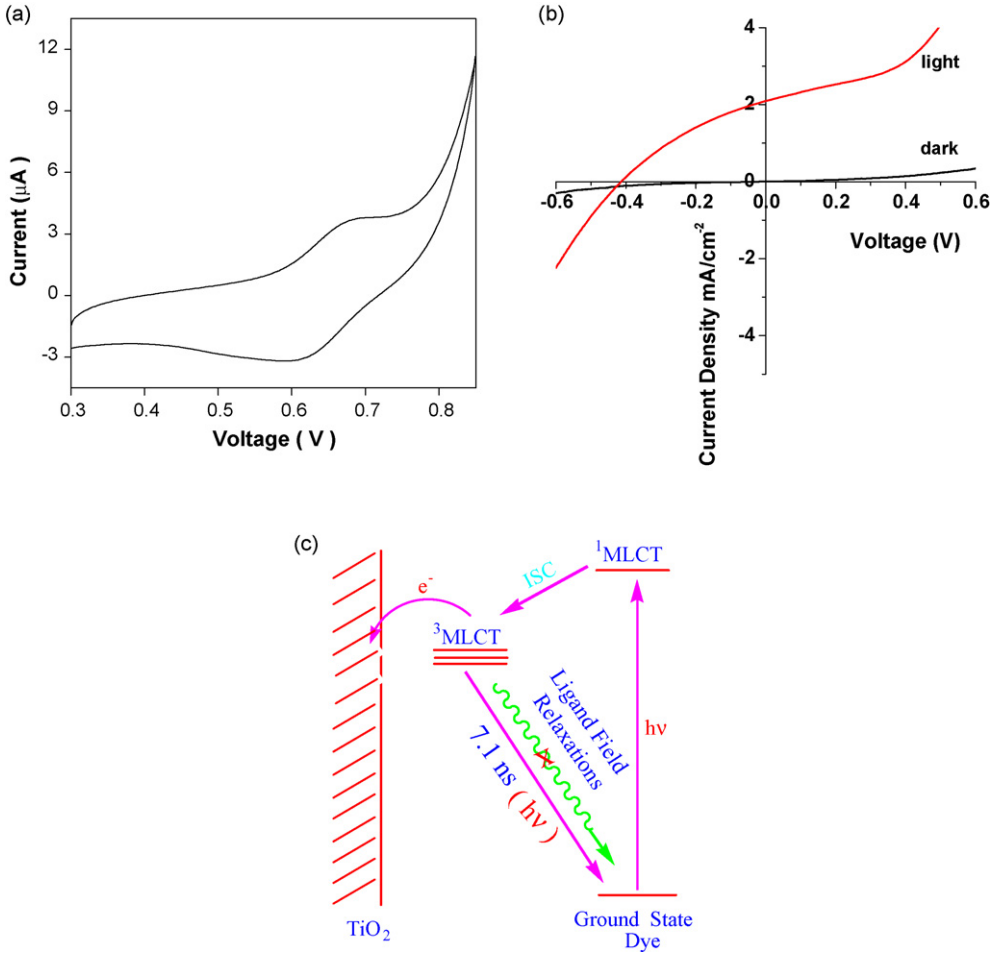

Fig. 3. (a) Cyclic voltammogram of a 2 mM solution of the complex in CH_3CN; supporting electrolyte 0.1 M n-Bu_4NPF_6; scan rate: 100 mV s^{-1}. (b) Current–voltage characteristics of the dye-sensitized solar cell in the presence and absence of light with the ruthenium complex as sensitizer. (c) Schematic description of the excited state manifold and the related photo-physical properties of ruthenium sensitizer.

and photo-current may be a consequence of charge carrier separation occurs within the complex and other components of the electrolyte [21]. Further extensive research is going in our laboratory to find the exact mechanistic pathway of the electron transfer within the dye component through photo-electrochemical measurements. The main objective of this work is to introduce the electron-withdrawing substituent like carboxylate in the terdendate ligand which can serve as anchoring group and as well as to maintain longer excited state lifetimes to undergo a very fast interfacial electron transfer processes.

4. Conclusion

In conclusion, we have successfully tuned the LUMO of the ruthenium sensitizer that show greater stabilization of the excited state and an energy conversion efficiency of 1.9%. Furthermore, this finding opens up the way to design more efficient sensitizers that have a high molar extinction coefficient, broad absorption in the near IR-region and a longer lifetime of the excited state by further modifying the ligand architecture to improve energy conversion efficiencies.

Acknowledgements

The research described herein was supported by the Department of Science and Technology, India (SR/FTP/CS-13/2005). The authors (RS and SA) thank Prof. Dr. M. Ashokkumar and Prof. Dr. Frances Separovic of University of Melbourne for the NMR and Mass analysis. The author (RS) thanks AICTE, New Delhi, for the NDF fellowship.

References

[1] M.K. Nazeeruddin, A. Kay, I. Rodicio, R. Humphry-Baker, E. Müller, P. Liska, N. Vlachopoulos, M. Grätzel, J. Am. Chem. Soc. 115 (1993) 6382–6390.
[2] M.K. Nazeeruddin, P. Pechy, M. Grätzel, Chem. Commun. (1997) 1705–1706.
[3] R. Argazzi, C. Bignozzi, T.A. Heimer, F.N. Castellano, G. Meyer, J. Inorg. Chem. 33 (1994) 5741–5749.
[4] A. Islam, H. Sugihara, M. Yanagida, K. Hara, G. Fujihashi, Y. Tachibana, R. Katoh, S. Murata, H. Arakawa, New J. Chem. 26 (2002) 966–968.
[5] T. Yamaguchi, M. Yanagida, R. Katoh, H. Sugihara, H. Arakawa, Chem. Lett. 33 (2004) 986–987.
[6] P. Maruthamuthu, S. Anandan, Sol. Energy Mater. Solar Cells 59 (1999) 199–209.
[7] S. Anandan, S. Latha, S. Murugesan, J. Madhavan, B. Muthuraaman, P. Maruthamuthu, Solar Energy 79 (2005) 440–448.
[8] V. Duprez, M. Biancardo, F.C. Krebs, Solar Energy Mater. Solar Cells 91 (2007) 230–237.
[9] A. Islam, F.A. Chowdhury, Y. Chiba, R. Komiya, N. Fuke, N. Ikeda, L. Han, Chem. Lett. 34 (2005) 344–345.
[10] A. Islam, F.A. Chowdhury, Y. Chiba, R. Komiya, N. Fuke, N. Ikeda, K. Nozaki, L. Han, Chem. Mater. 18 (2006) 5178–5185.
[11] D.L. Jameson, J.K. Blaho, K.T. Kruger, K.A. Goldsby, Inorg. Chem. 28 (1989) 4312–4314.
[12] T. Stergiopoulos, S. Karakotas, P. Falaras, J. Photochem. Photobiol. A: Chem. 163 (2004) 331–340.
[13] E.A. Medlycott, G.S. Hanan, Chem. Soc. Rev. 34 (2005) 133–142.
[14] T. Vermonden, D. Branowska, A.T.M. Marcelis, E.J.R. Sudhölter, Tetrahedron 59 (2003) 5039–5045.
[15] N. Garelli, P. Vierling, J. Org. Chem. 57 (1992) 3046–3051.
[16] K. Chryssou, V.J. Catalano, R. Kurtaran, P. Falaras, Inorg. Chim. Acta 328 (2002) 204–209.

[17] K. Chryssou, T. Stergiopoulos, P. Falaras, Polyhedron 21 (2002) 2773–2781.
[18] A.I. Philippopoulos, A. Terzis, C.P. Raptopoulou, V.J. Catalano, P. Falaras, Eur. J. Inorg. Chem. (2007) 5633–5644.
[19] S. Anandan, S. Latha, P. Maruthamuthu, J. Photochem. Photobiol. A: Chem. 150 (2002) 167–175.
[20] T.A. Heimer, E.J. Heilweil, C.A. Bignozzi, G.J. Meyer, J. Phys. Chem. A 104 (2000) 4256–4262.
[21] K. Hara, T. Nishikawa, M. Kurashige, H. Kawauchi, T. Kashima, K. Sayama, K. Aika, H. Arakawa, Solar Energy Mater. Solar Cells 85 (2005) 21–30.